Chapter 14
In Silico Biofluid Mechanics

Copyright © 2015 Elsevier Inc. All rights reserved.

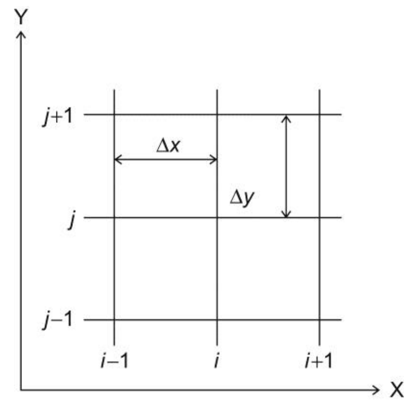

Figure 14.1 Two-dimensional (2D) grid for the FDM, where *i* denotes grid spaces in the *x*-direction and *j* denotes grid spaces in the *y*-direction. Note that the spacing does not have to be uniform across the entire geometry. By using either the forward difference method or the backward difference method, parameters of interest can be obtained from known boundary conditions and known initial conditions.

Copyright © 2015 Elsevier Inc. All rights reserved.

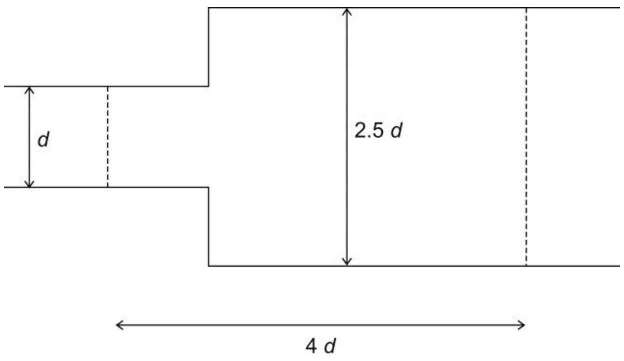

Figure 14.2 Idealized flow in a sudden expansion from the microcirculation to the venous system. Clearly, based on the geometry, the computational results will differ, but with simple geometries an idea of the flow field can be established.

Copyright © 2015 Elsevier Inc. All rights reserved.

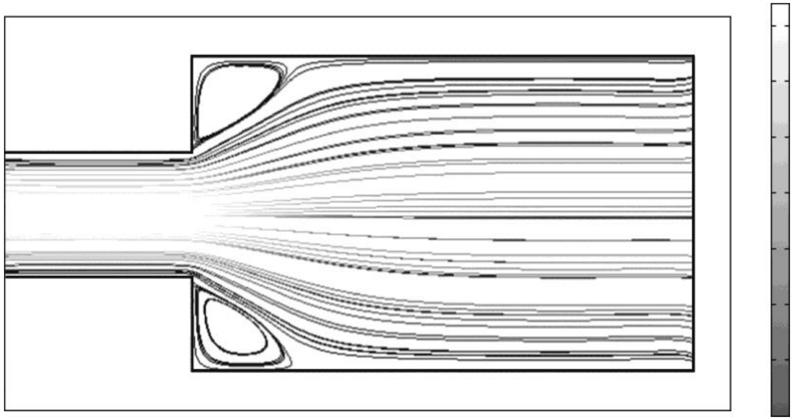

Figure 14.3 Computational fluid dynamic solution for the flow conditions in Figure 13.2. This illustrates that in a sudden expansion, there will be a stagnation zone in which the fluid becomes trapped.

Copyright © 2015 Elsevier Inc. All rights reserved.

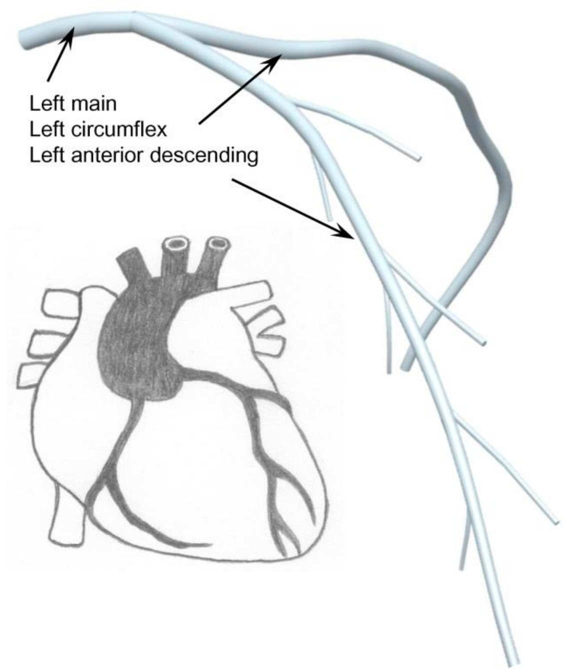

Figure 14.4 A three-dimensional (3D) model of the left coronary artery with branches, generated by Pro-Engineering software. This geometry can be imported into most CFD software for flow field (velocity vectors, pressure, among others) computation.

Copyright © 2015 Elsevier Inc. All rights reserved.

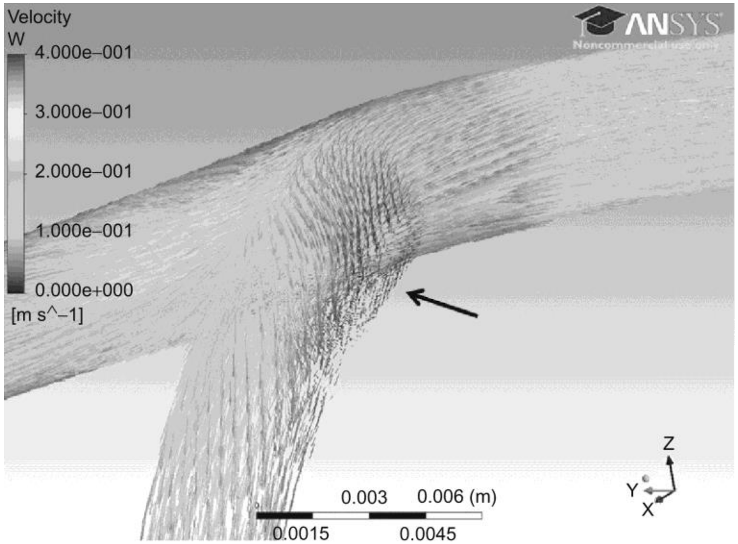

Figure 14.5 Velocity vectors in the left coronary artery near the bifurcation. Due to flow separation at the bifurcation, a recirculation zone developed (arrow), which can potentially trap cells and induce abnormal shear stresses.

Copyright © 2015 Elsevier Inc. All rights reserved.

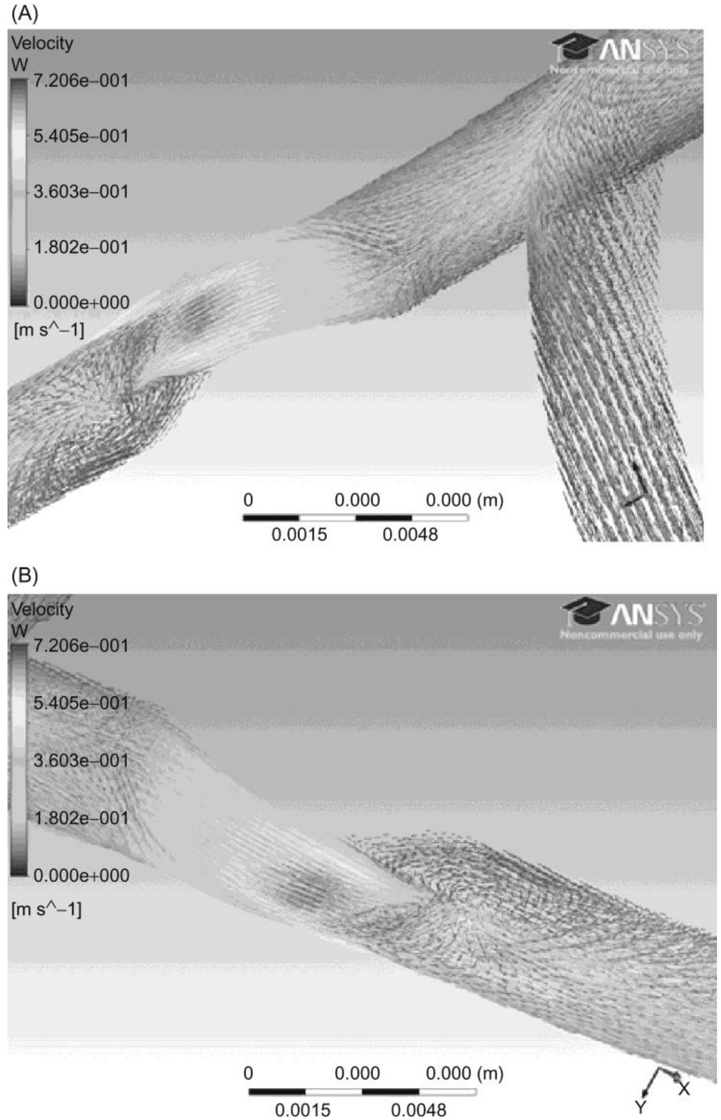

Figure 14.6 Velocity vectors in the left descending artery with an 80% stenosis (A). Jet flow developed at the stenosis throat, inducing a large recirculation zone distal to the stenosis. The recirculation zone by the bifurcation upstream is still visible. A close-up view of the stenosis and the recirculation zone is shown in (B).

Copyright © 2015 Elsevier Inc. All rights reserved.

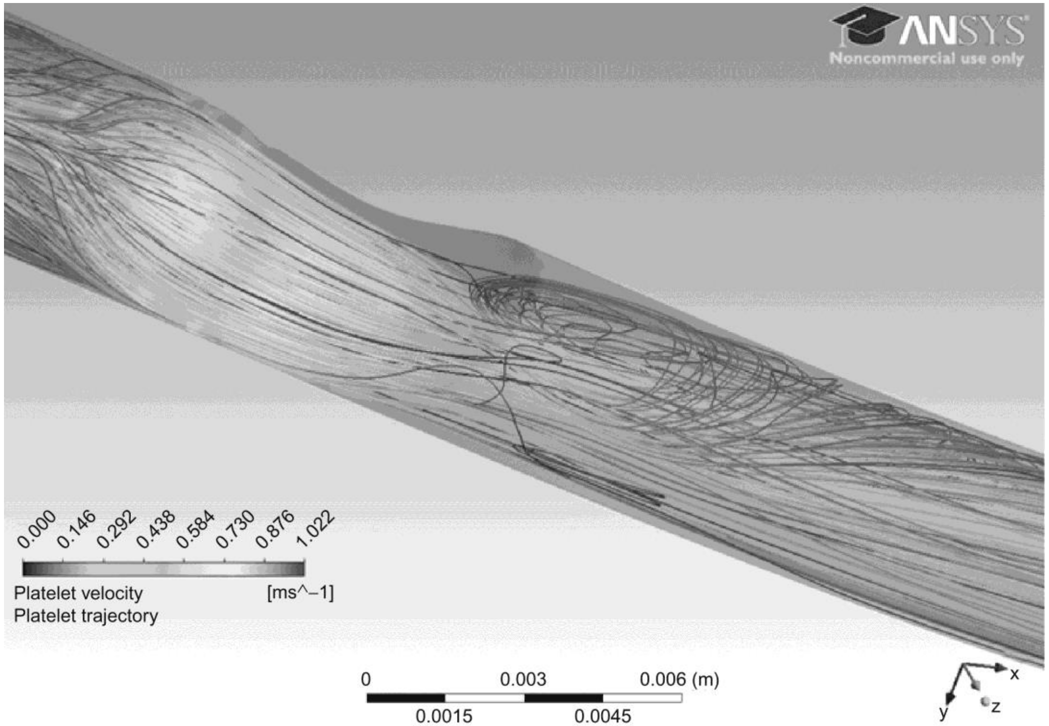

Figure 14.7 A discrete-phase model can be used to estimate platelet trajectories after they pass an 80% stenosis in the left descending artery. This image shows the trajectories of every particle seeded at the inlet and we can see that a significant proportion of these become trapped in the recirculation zone downstream of the stenosis.

Copyright © 2015 Elsevier Inc. All rights reserved.

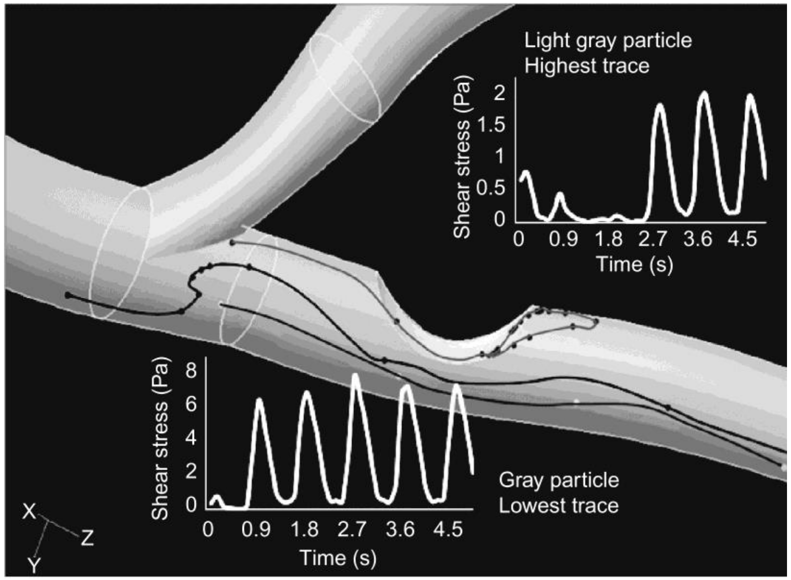

Figure 14.8 The shear stress history of platelets within the left coronary model estimated using the Boussinesq approximation, following their trajectories for five cardiac cycles. The two exported shear stress histories are for the lowest trace (gray particle) and the highest trace (light gray particle).

Copyright © 2015 Elsevier Inc. All rights reserved.

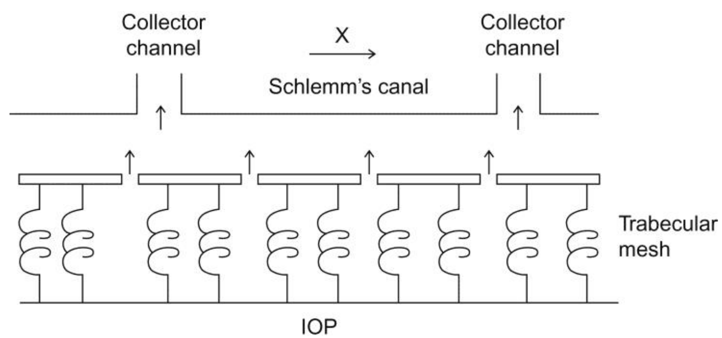

Figure 14.9 Model of Schlemm's canal for in-text example. *Source: Adapted from John and Kamm*.

Copyright © 2015 Elsevier Inc. All rights reserved.

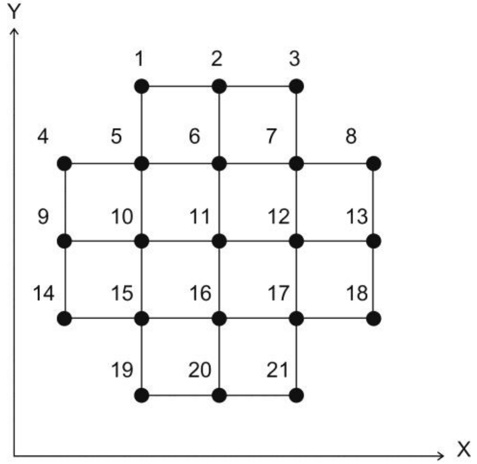

Figure 14.10 Grid for homework problem 14.1.

Copyright © 2015 Elsevier Inc. All rights reserved.